Water ice on Kuiper Belt object 1996 TO/sub 66/

Brown, R.H.; Cruikshank, D.P.; Pendleton, Y.
Lunar & Planetary Lab., Arizona Univ., Tucson, AZ, USA

Astrophysical Journal, Letters , vol.519, no.1, pt.2 , Page: L101-4
Publisher: University of Chicago Press for American Astron. Soc , 1 July 1999
Language: English

Abstract: The 1.40-2.45 mu m spectrum of Kuiper Belt object 1996 TO/sub 66/ was measured at the Keck Observatory in 1998 September. Its spectrum shows the strong absorptions near 1.5 and 2.0 mu m that are characteristic of water ice-the first such detection on a Kuiper Belt object. The depth of the absorption bands and the continuum reflectance of 1996 TO/sub 66/ suggest the presence of a black to slightly blue-colored, spectrally featureless particulate material as a minority component mixed with the water ice. In addition, there is evidence that the intensity of the water bands in the spectrum of 1996 TO/sub 66/ varies with rotational phase, suggesting a "patchy" surface. (19 References)

Subjects:
asteroids
astronomical spectra
ice
infrared astronomy
planetary surfaces
Experimental
chemical composition
surface
water ice
asteroid
Kuiper Belt object
1996 TO/sub 66/
infrared spectrum
IR spectra
strong absorption
AD 1998 09
continuum reflectance
black matter
blue
particulate material
patchy surface
1.4 to 2.45 mum
H/sub 2/O
Asteroids
Infrared astronomical observations
Planetary surfaces and topography; tectonics
Planetary chemical composition

Abstract

The 1.40-2.40 μm spectrum of Kuiper Belt object (KBO) 1996 TO_{66} was measured at the Keck Observatory in September 1998. It's spectrum shows the strong absorptions near 1.5 and 2.0 μm characteristic of water ice--the first such detection on a Kuiper Belt object. The depth of the absorption bands and the continuum reflectance of 1996 TO_{66} also suggest the presence of a black to slightly blue-colored, spectrally featureless particulate material as a minority component mixed with the water ice. In addition, there is evidence that the intensity of the water bands in the spectrum of 1996 TO_{66} vary with rotational phase suggesting that it has a "patchy" surface.

It is becoming increasingly clear that the remnant population of objects just beyond the orbit of Neptune is indeed representative of the small bodies (planetesimals) from which the planets accreted(*1,2*). Kuiper Belt objects (KBOs), as they are sometimes called, are mostly beyond the range of planetary perturbations and too tightly bound to the Sun to be perturbed by passing stars (*1,2*). Thus KBOs are thought to be primitive remnants of the early solar system (*1,2*), and may have unique surface compositional characteristics.

Studies of the physical properties and surface compositions of bodies in the outer solar system can give important clues to conditions existing in the early solar system. At the great heliocentric distances of the outer solar system, materials there are expected to be less modified by solar heating than materials in the region of the terrestrial planets. Thus, small bodies in the outer solar system are thought to preserve a more accurate record of the chemical and physical properties of the original material from which the solar system formed. Because our understanding of early solar system chemistry depends upon our knowledge of the small bodies in the outer solar system, an important suite of bodies to study are the KBOs.

We report here near-infrared spectroscopy of the Kuiper Belt object 1996 TO_{66}, and discuss its implications. The data were obtained at the W. M. Keck Observatory on September 27 and 28, 1998 (universal time), using the Near Infrared Camera (NIRC). The measurements were made using the gr120 grism of the NIRC which has an approximate wavelength range in first order of 1.35-2.55 μm and a spectral sampling interval of 0.00607 μm per pixel. The NIRC has an effective pixel size of 0.15 arcsec, and a slit width of 8.5 pixels (~1.3 arcsec) was used for all the spectral observations. Atmospheric seeing on the night in question was about 0.5 arcsec (full width at half maximum) at 2.2 μm.

1996 TO_{66} was identified in images taken through the NIRC's K_s filter (*3*), both by its motion, as well as by its predicted position on the sky. Spectra were collected by centering the image of the object in the grism slit and obtaining pairs of images of 1200 sec total exposure (15 separate exposures of 80 seconds co-added) with each exposure offset along the grism slit by 12 arcsec. A first-order subtraction of the sky background was accomplished by subtracting corresponding image pairs. Our spectra of 1996 TO_{66} encompass 4800 seconds of integration on each of 2 nights.

Correction for telluric extinction and the solar color was accomplished by using spectra of the C-type asteroid 329 Svea obtained on the same night and over the same airmass range (1.03-1.13). 329 Svea was chosen because it has a flat spectrum with no spectral features over the wavelength range of the observations presented here (*4,5*).

The resultant spectra are shown in Figure 1, convolved to lower resolution to enhance the signal-to-noise ratio (*6*). The data are in good agreement with the broadband colorimetry of 1996 TO_{66} reported by Jewitt and Luu (*7*). Readily apparent in the spectra from both nights are strong absorption bands near 1.5 and 2.0 μm. It can also be seen that the intensities of the absorptions near 1.5 and 2.0 μm substantially differ across the two nights' data, suggesting that varying areal coverage and/or concentration of the absorbing material is revealed as the object rotates. The two absorptions near 1.5 and 2.0 μm are attributed to water ice on the surface of 1996 TO_{66}. To illustrate this, in Figure 2 we show the average of both nights data at full resolution, and the data convolved to lower resolution in the same manner as the spectra shown in Fig. 1. Also shown in Fig. 2 is a model spectrum of particulate water ice intimately mixed with neutral to bluish, but otherwise spectrally featureless, particulate material. The model spectrum (*8*) was calculated using bidirectional reflectance theory (*9*), the known optical constants of water ice (*10-12*) and a simulated dark material that is spectrally featureless but blue colored over the wavelength region of our observations (*13*) . As can be clearly seen, both the model and the data show the strong 1.52- and 2.03 μm absorption of water ice. The spectral match is strong enough that we consider water ice to be positively identified on the surface of 1996 TO_{66}. The simulated dark material in our model was chosen merely to improve the fit in 1.4-2.4 μm spectral region. Whether the surface of 1996 TO_{66} actually contains material similar in color to the material used in our simulation cannot be uniquely determined from these data.

Although the model fits reasonably well, there are two rather significant discrepancies. The first is an apparent absorption band near 1.8 μm, the second is a mismatch between the model spectrum and the data beyond 2.2 μm. The apparent absorption near 1.8 μm is also seen in the spectrum of 1993 SC (*13*). To account for this absorption, if real, would require an additional molecular component of the surface of 1996 TO_{66} besides H_2O. Nevertheless, we cannot be certain whether the absorption is real or an artifact of incomplete extinction correction in the neighborhood of the strong 1.9 μm telluric water vapor absorption.

The mismatch between the model and the data beyond 2.2 μm is a bit more interesting because there are no strong telluric absorptions in the 2.2-2.4 μm wavelength region, suggesting that the drop in reflectance of the data relative to the model is real. It is not clear from these data whether the discrepancy is due to another molecular component on 1996 TO_{66} or a difference in the actual optical constants of the water on 1996 TO_{66} versus those measured in the laboratory *(9-11)*.

Notable also, is the weakness or absence of the 1.65 μm absorption that is partially blended with the 1.52 μm absorption in crystalline water ice (*14*). The weakness or absence of this band in our data is consistent with amorphous water ice, rather than crystalline water ice on 1996 TO_{66}, although certainty demands more precise data.

It is interesting that the spectrum of the Centaur 1997 CU_{26} (*15*), shows water-ice absorptions and little else except red, spectrally featureless material. In contrast, a well-studied Centaur Pholus (*16*), shows an absorption band at 2.03 μm attributed to water ice on its surface, and its overall red color has been attributed to the presence of red, organic material (*16-18*). Pholus also shows evidence of light organic compounds such as methanol (CH_3OH) (*16*). The spectrum of the KBO 1993 SC (*13*) shows evidence for light hydrocarbons on its surface, but none for water ice. Finally, Chiron, another Centaur whose orbit crosses that of Saturn and Uranus, has a weak coma and undergoes episodic gas releases like a comet. Its spectrum from 1.4-2.4 μm is featureless and nearly flat, similar to that of a C-type asteroid (*19*).

The spectral differences and similarities among the Kuiper Belt objects and the Centaurs suggest both populations are compositionally diverse groups of objects. Many recent studies of solar system dynamics conclude that the Kuiper Belt is the source of the Centaurs and the short period comets (*20*). The data presented here and the spectral evidence gathered to date (though sparse) are supportive of that view.

ACKNOWLEDGEMENTS. The W. M. Keck Observatory is operated as a scientific partnership between the California Institute of Technology and the University of California. It was made possible by the generous financial support of the W. M. Keck Foundation. The authors acknowledge the assistance of Josh Emery at the telescope, and the support of the U. S. National Aeronautics and Space Administration through the various grants and contracts that support the authors' work.

References and Notes

1. G. P. Kuiper, In *Astrophysics*, J. A. Hynek, Ed. (McGraw Hill, New York, 1951), pp. 357-424
2. K. E. Edgeworth, *MNRAS*, **109**, 600 (1948).
3. K_s is a filter whose passband encompasses the short wavelength half of the standard K band and is centered at approximately 2.12 μm.
4. D. J. Tholen, In Asteroids II (University of Arizona Press, Tucson) pp. 1139-1150 (1989).
5. J. F. Bell, B. R. Hawke, P. D. Owensby, and M. J. Gaffey, LPSC XIX, p. 57 (1988).
6. The convolution to lower resolution was done as a pure, discrete convolution. The purpose is to model how the data would look if obtained at intrinsically lower spectral resolution (with the associated increase in S/N ratio due to the larger spectral bandpass). Most grating spectrometers have Gaussian bandpasses, thus we used a Gaussian convolution. In addition, using a Gaussian bandpass eliminates the Fourier spectral aliasing that would occur if one simply used a square bandpass to bin the data (i.e., convolve the spectrum with a square wave).
7. D.C. Jewitt and J.X. Luu, *Astron. J.*, **115**, 1667 (1998).
8. The grain sizes of the water ice and spectrally featureless material used in the model are 68 μm and 160 μm respectively. These values are not unique and one should not ascribe any great significance to them because the abundances and grains sizes of the two constituents can be varied within a wide range and still provide an acceptable match to the water-ice absorption bands in the spectrum.
9. B. Hapke, In *Remote Geochemical Analyses: Elemental and Mineralogical Composition* (Cambridge University Press, New York, 1993), pp. 31-41.
10. S. Warren, *Applied Optics* **23**, 1206 (1984).
11. O. B. Toon, M. A. Tolbert, B. G. Koehler, A. M. Middlebrook, and J. Jordan, *JGR* **99**, 25631.

12. The optical constants of water ice used in the spectral models here were taken from Warren (*8*) and shifted in wavelength to agree with the data of Toon et al. (*9*). The data of Warren were deemed to be more precise in the 1.4-2.4 μm wavelength region than those of Toon, but the central wavelengths of the absorption bands in the Toon data corresponded more closely with those of water ice at the expected surface temperature of 1996 TO_{26}.

13. The optical constants for the blue material used here were derived by assuming a real index of refraction of 1.6 in the visual spectral region, and assuming a Lambert absorption coefficient that decreased linearly toward longer wavelengths. These quantities then served as inputs to a subtractive Kramers-Kronig algorithm which gave the spectrum of real indices of refraction corresponding to the defined imaginary indices and the real index in the visual. The calculated reflectance for 10 μm grains gives a roughly linear decrease in reflectance from 10% at 1.0 μm to 7 % at 2.5 μm.

14. R. H. Brown, D. P. Cruikshank, Y. Pendleton, and G. D. Veeder, *Science* **276,** 937-939 (1997).

15. U. Fink and G. T. Sill, In *Comets* (L. Wilkening Ed.), University of Arizona Press, Tucson, pp. 164-202.

16. R. H. Brown, D. P. Cruikshank, Y. Pendleton, and G. D. Veeder, *Science* **280,** 1430-1432 (1998).

17. D. P. Cruikshank et al., *Icarus* **135,** 389 (1998).

18. C. Sagan, B. N. Khare and J. S. Lewis, In *Satellites* (J. A. Burns and M. S. Matthews, Eds.), University of Arizona Press, Tucson, pp. 788-807 (1984).

19. D. P. Cruikshank, In *From Stardust to Planetesimals* (Y. J. Pendleton and A. G. G. M. Tielens, Eds.), A.S.P Conference Proceedings **122,** pp. 315-333 (1997)

20. M. Duncan, T. Quinn, and S. Tremaine, *Astrophys. J. Lett.* **328,** L69 (1988); B. Gladman and M. Duncan, *Astron. J.*, **100**, 1680 (1990); M. J. Holman and J. Wisdom, *Astron. J.*, **105**, 1987 (1993); M. Irwin, S. Tremaine, and A. Zytkow, *Astron. J.*, **110**, 3082 (1995); D. Jewitt, J. Luu, and J. Chen, *Astron. J.*, **112**, 1225 (1996); J. Luu, D. Jewitt, and E. Cloutis, *Icarus* **109**, 133 (1994).

Figure 1: Spectra of 1996 TO_{66}. The data have been convolved to lower resolution to improve the S/N ratio (*6*). The data in the upper panel are from Sept. 27, 1998, and the data in the lower panel are from Sept. 28, 1998 (see text).

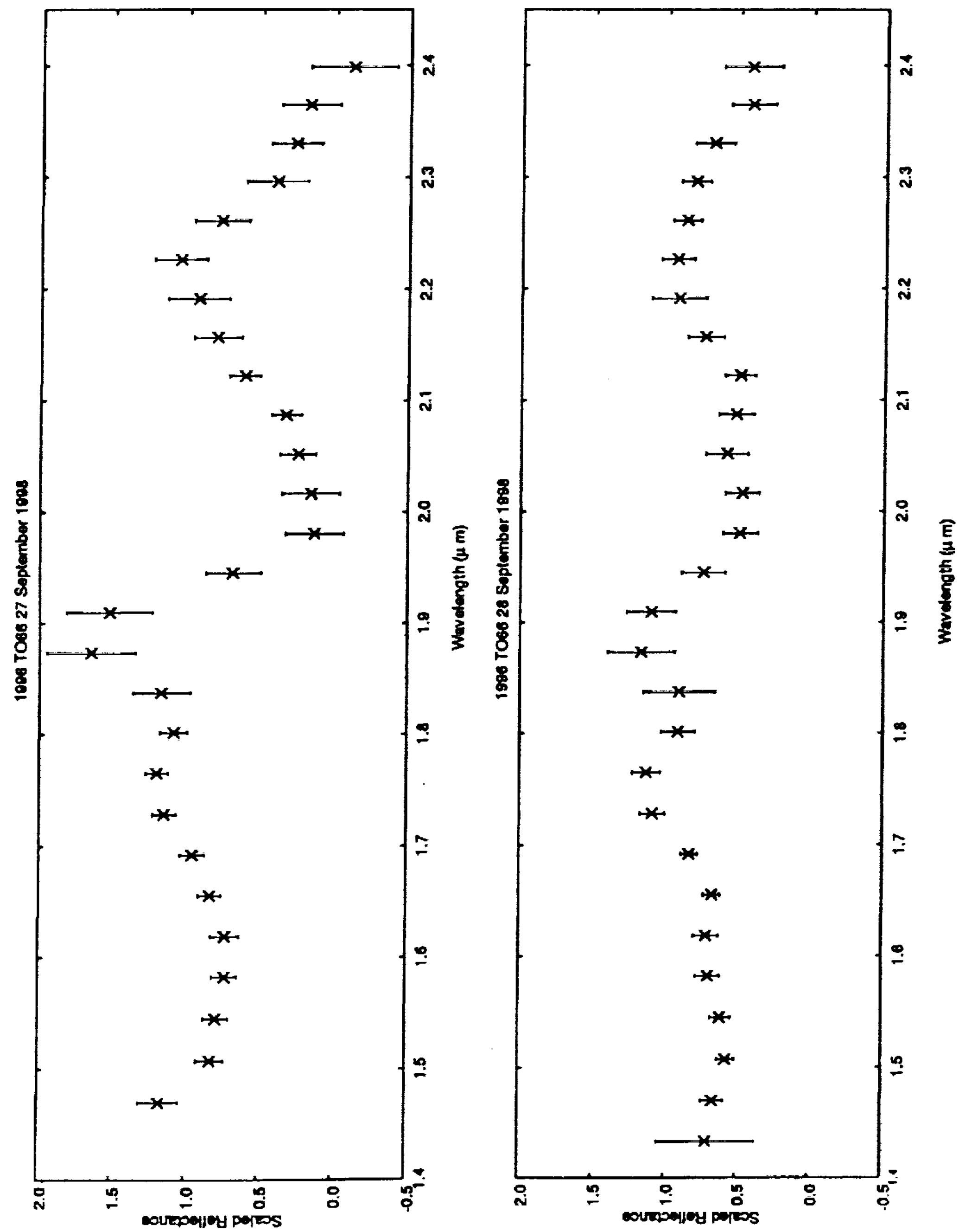

Figure 2: Spectra of 1996 TO_{66} from both nights data averaged together. The data in the lower panel are at full resolution and the data in the upper panel have been convolved to lower resolution (*6*). A model was fit to the data and is represented by the solid line (see text).